

## Borylene-Based Direct Functionalization of Organic Substrates: Synthesis, Characterization, and Photophysical Properties of Novel $\pi$ -Conjugated Borirenes

Holger Braunschweig,\* Thomas Herbst, Daniela Rais, Sundargopal Ghosh, Thomas Kupfer, and Krzysztof Radacki

*Institut für Anorganische Chemie, Bayerische Julius-Maximilians-Universität Würzburg Am Hubland, 97 074 Würzburg, Germany*

Andrew G. Crawford, Richard M. Ward, and Todd B. Marder\*

*Department of Chemistry, Durham University, South Road, Durham, DH1 3LE, U.K.*

Israel Fernández\*

*Dpto. Química Orgánica I, Universidad Complutense de Madrid, 28040 Madrid, Spain*

Gernot Frenking\*

*Fachbereich Chemie, Philipps-Universität Marburg, Hans-Meerwein-Strasse, 35043 Marburg, Germany*

Received March 30, 2009; E-mail: H.Braunschweig@mail.uni-wuerzburg.de; Frenking@chemie.uni-marburg.de; Israel@quim.ucm.es; Todd.Marder@durham.ac.uk

**Abstract:** Room temperature photolysis of aminoborylene complexes, [(CO)<sub>5</sub>M=B=N(SiMe<sub>3</sub>)<sub>2</sub>] (**1**: M = Cr, **2**: Mo) in the presence of a series of alkynes and diynes, 1,2-bis(4-methoxyphenyl)ethyne, 1,2-bis(4-(trifluoromethyl)phenyl)ethyne, 1,4-diphenylbuta-1,3-diyne, 1,4-bis(4-methoxyphenyl)buta-1,3-diyne, 1,4-bis(trimethylsilylethynyl)benzene and 2,5-bis(4-*N,N*-dimethylaminophenylethynyl)thiophene led to the isolation of novel mono and bis-bis-(trimethylsilyl)aminoborirenes in high yields, that is [(RC=CR)( $\mu$ -BN(SiMe<sub>3</sub>)<sub>2</sub>)] (**3**: R = C<sub>6</sub>H<sub>4</sub>-4-OMe and **4**: R = C<sub>6</sub>H<sub>4</sub>-4-CF<sub>3</sub>); [{"( $\mu$ -BN(SiMe<sub>3</sub>)<sub>2</sub>(RC=C-))<sub>2</sub>}] (**5**: R = C<sub>6</sub>H<sub>5</sub> and **6**: R = C<sub>6</sub>H<sub>4</sub>-4-OMe); [1,4-bis-{( $\mu$ -BN(SiMe<sub>3</sub>)<sub>2</sub>(SiMe<sub>3</sub>C=C))}benzene], **7** and [2,5-bis-{( $\mu$ -BN(SiMe<sub>3</sub>)<sub>2</sub>(C<sub>6</sub>H<sub>4</sub>NMe<sub>2</sub>-C=C)}-thiophene], **8**. All borirenes were isolated as light yellow, air and moisture sensitive solids. The new borirenes have been characterized in solution by <sup>1</sup>H, <sup>11</sup>B, <sup>13</sup>C NMR spectroscopy and elemental analysis and the structural types were unequivocally established by crystallographic analysis of compounds **6** and **7**. DFT calculations were performed to evaluate the extent of  $\pi$ -conjugation between the electrons of the carbon backbone and the empty p<sub>z</sub> orbital of the boron atom, and TD-DFT calculations were carried out to examine the nature of the electronic transitions.

### Introduction

Boron-containing molecular and polymeric species have remarkable linear, nonlinear and electro optical properties, and have had a significant impact in the area of materials chemistry.<sup>1–3</sup>  $\pi$ -Conjugated organic compounds, in particular, displaying three coordinate boron centers, constitute a highly topical area of research, as these functional molecular and polymeric materials have potential for applications in OLEDs,

sensors, solar cells and electronic circuits.<sup>1</sup> Three coordinate boron based materials, for which a variety of structural patterns have been realized, have the presence of trivalent, sp<sup>2</sup>-hybridized boryl groups in common. Hence, their generation relies on conventional synthetic techniques common in organoboron chemistry,<sup>4–6</sup> for example, hydro- and diboration of C–C multiple bonds, salt elimination and silicon–boron exchange. Based on recent work in our laboratory, it was demonstrated

- (1) (a) Entwistle, C. D.; Marder, T. B. *Angew. Chem., Int. Ed.* **2002**, *41*, 2927–2931. (b) Entwistle, C. D.; Marder, T. B. *Chem. Mater.* **2004**, *16*, 4574–4585. (c) Jäkle, F. *Coord. Chem. Rev.* **2006**, *250*, 1107–1121. (d) Elbing, M.; Bazan, G. C. *Angew. Chem., Int. Ed.* **2008**, *47*, 834–838.
- (2) (a) Noda, T.; Ogawa, Y. S.; Shirota, Y. *Adv. Mater.* **1999**, *11*, 283–285. (b) Shirota, Y.; Kinoshita, T.; Noda, K.; Okumoto, T. O. *J. Am. Chem. Soc.* **2000**, *122*, 11021–11022. (c) Matsumi, N.; Naka, K.; Chujo, Y. *J. Am. Chem. Soc.* **1998**, *120*, 5112–5113. (d) Li, H.; Sundararaman, A.; Venkatasubbaiah, K.; Jäkle, F. *J. Am. Chem. Soc.* **2007**, *129*, 5792–5793. (e) Zhao, C.-H.; Wakamiya, A.; Inukai, Y.; Yamaguchi, S. *J. Am. Chem. Soc.* **2006**, *128*, 15934–15935.

- (3) (a) Wakamiya, A.; Mori, K.; Yamaguchi, S. *Angew. Chem., Int. Ed.* **2007**, *46*, 4273–4276. (b) Qin, Y.; Cheng, G.; Achara, O.; Parab, K.; Jäkle, F. *Macromolecules* **2004**, *37*, 7123–7131. (c) Parab, K.; Quin, Y.; Jäkle, F. *Poly. Mater. Sci. Eng. Prepr.* **2005**, *93*, 422. (d) Haussler, M.; Tang, B. Z. *Adv. Polym. Sci.* **2007**, *209*, 1–58.
- (4) (a) Brown, H. C. *Hydroboration*; Wiley-Interscience: New York, 1962. (b) Brown, H. C. *Boranes in Organic Chemistry*; Cornell University Press: Ithaca, 1972. (c) Onak, T. *Organoborane Chemistry*; Academic Press: New York, 1975. (d) Beletskaya, I.; Pelter, A. *Tetrahedron* **1997**, *53*, 4957–5026.
- (5) (a) Marder, T. B.; Norman, N. C. *Top. Catal.* **1998**, *5*, 63–73. (b) Han, L.-B.; Tanaka, M. *Chem. Commun.* **1999**, 395–402. (c) Ishiyama, T.; Miyaura, N. *J. Organomet. Chem.* **2000**, *611*, 392–402.

that borylene complexes of the type  $[L_xM=B=NR_2]$  ( $M = Cr, Mo, W$ ;  $R = SiMe_3$ )<sup>7–10</sup> not only stabilize borylenes in the coordination sphere of various transition metals but, more importantly, serve as unprecedented sources for the elusive BR moiety, under mild conditions.<sup>11,12</sup>

Borylenes represent hypovalent, low coordinate species which, unlike their low valent carbon relatives, carbenes  $CR_2$ , are highly reactive compounds that cannot be generated or handled under standard conditions. Classical studies by Timms proved that B–F can be generated at high temperature >2000 °C in dilute gas phase,<sup>13</sup> and B–SiPh<sub>3</sub> was obtained photochemically in hydrocarbon matrices at –196 °C by West.<sup>14</sup> Some notable accounts on this novel class of organometallics followed,<sup>15–18</sup> but development has been slow because convenient routes to these compounds were not available and, owing to the drastic conditions under which borylenes are accessible as short-lived species, the chemistry of these compounds has been severely limited.

Having developed a practical synthetic route to borylene complexes of group 6 metals  $[(CO)_nM=B=N(SiMe_3)_2]$ , (**1**:  $M = Cr$ , **2**:  $Mo$ ) in good yields, a variety of reactivity patterns were investigated. Reactions with cyclopentadienylmetallocarbonyls of groups 8–9 and with alkynes have been found to be the most profitable.<sup>10–12,19–21</sup> The results prior to this work are shown in Scheme 1 and illustrate the thermal and photochemical transfer of borylene ligands from borylene complexes to inorganic (Scheme 1a–b) and organic species (Scheme 1c).

Boracyclopropenes or borirenes are isoelectronic with cyclopropenium cations, that is, the smallest aromatic carbocycles

that might exhibit  $2\pi$  aromatic stabilization, and have attracted considerable fundamental interest; however, synthetic methods yielding borirenes are laborious, low yielding, and severely limited in scope.<sup>22</sup> Herein, we report the photochemical transfer of the aminoborylene moiety,  $BN(SiMe_3)_2$  from  $[(CO)_nM=B=N(SiMe_3)_2]$ , ( $M = Cr$  and  $Mo$ ) to a set of selected alkynes and diynes, which led to the isolation of novel  $\pi$ -conjugated borirenes, all of which have been characterized spectroscopically as well as, in selected cases, by X-ray diffraction studies. This borylene based functionalization of carbon–carbon triple bonds turned out to be not only applicable to a wide range of substrates including alkynes and diynes, but also to proceed with very high yield. Upon availability of these borirenes in sufficient quantities, theoretical calculations combined with spectroscopic data were employed to elucidate the electronic structure of these species particularly with respect to the extent of  $\pi$ -delocalization within the BCC-ring.

## Results and Discussions

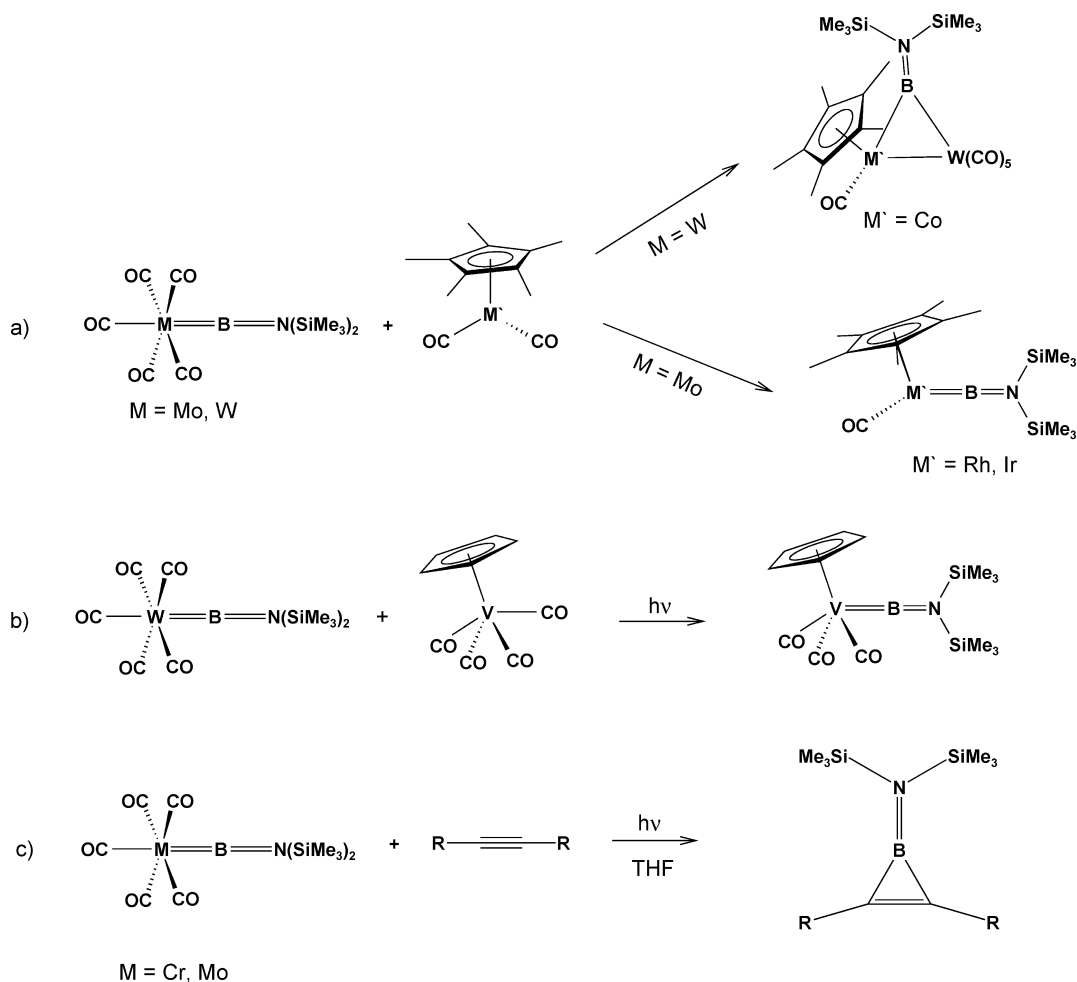
**Synthesis and Characterization of Mono- and Bis-bis(trimethylsilyl)aminoborirenes, 3–8 by Photochemical Borylene Transfer from  $[(CO)_5M=B=N(SiMe_3)_2]$  ( $M = Cr, Mo$ ).** As shown in Scheme 2, UV irradiation of a pale-yellow solution of  $[(CO)_5M=B=N(SiMe_3)_2]$ , (**1**:  $M = Cr$  and **2**:  $Mo$ ) in THF with appropriate quantities of the alkynes 1,2-bis(4-methoxyphenyl)ethyne, 1,2-bis(4-(trifluoromethyl)phenyl)ethyne, 1,4-diphenylbuta-1,3-diyne, 1,4-bis(4-methoxyphenyl)buta-1,3-diyne, 1,4-bis(trimethylsilylethynyl)benzene and 2,5-bis(4-*N,N*-dimethylamino-phenylethynyl)thiophene, for 4–8 h at room temperature resulted in the formation of mono and bis-borirenes, **3–8**. All reactions were monitored by multinuclear NMR spectroscopy, which revealed gradual consumption of the starting materials and quantitative formation of the new boron containing compounds, as indicated by the presence of a singlet resonance in the  $^{11}B\{^1H\}$  NMR spectrum at  $\delta$  23.7–29.1 ppm.

$[(RC=CR)(\mu-BN(SiMe_3)_2)]$ . (**3**:  $R = C_6H_4-4-OMe$  and **4**:  $R = C_6H_4-4-CF_3$ ): Room temperature photolysis of a pale yellow solution of  $[(CO)_5Cr=B=N(SiMe_3)_2]$ , **1** in the presence of 1,2-bis(4-methoxyphenyl)ethyne or 1,2-bis(4-trifluoromethylphenyl)ethyne for 4 h led to the isolation of **3** and **4**, respectively. In both cases, aminoborirenes have been isolated almost in quantitative yields in the form of pale yellow crystals by filtration of the reaction mixture and subsequent crystallization from hexane at –60 °C. Compounds **3** and **4** have been characterized by comparison of their spectroscopic data with those of related compounds.<sup>23</sup> The  $^{11}B\{^1H\}$  NMR spectra of **3** and **4** show the presence of a single resonance at  $\delta = 25$  and 27 ppm, respectively. These values are in good agreement with those reported by Habben and Meller for a series of 1-bis(trimethylsilyl)aminoborirenes<sup>24</sup> which appeared at  $\delta = 26.5–27.7$  ppm. The mass spectrometric data for **3** and **4** suggest molecular formulas  $[(MeOC_6H_4CCC_6H_4OMe)BN(SiMe_3)_2]$  and  $[(CF_3C_6H_4CCC_6H_4CF_3)BN(SiMe_3)_2]$ , respectively. The  $^1H$  NMR spectra show a single resonance for the N-( $SiMe_3$ )<sub>2</sub> protons at  $\delta = 0.31$  ppm, indicating a symmetric structure.

- (6) (a) Cragg, G. M. L. *Organoboranes in Organic Synthesis*; Marcel Dekker: New York, 1972. (b) Suzuki, A.; Miyaura, N. *Chem. Rev.* **1995**, *95*, 2457–2483. (c) Kaufmann, D. E.; Matteson, D. S. *Science of Synthesis*; Boron Compounds; Thieme: Stuttgart, 2005; Vol. 6.
- (7) (a) Braunschweig, H. *Angew. Chem., Int. Ed.* **1998**, *37*, 1786–1801. (b) Braunschweig, H.; Kollann, C.; Englert, U. *Angew. Chem., Int. Ed.* **1998**, *37*, 3179–3180.
- (8) Braunschweig, H.; Colling, M. *Eur. J. Inorg. Chem.* **2003**, 393–403.
- (9) Braunschweig, H. *Adv. Organomet. Chem.* **2004**, *51*, 163–192.
- (10) Blank, B.; Braunschweig, H.; Colling-Hendelkens, M.; Kollann, C.; Radacki, K.; Rais, D.; Uttinger, K.; Whittell, G. R. *Chem.–Eur. J.* **2007**, *13*, 4770–4781.
- (11) Braunschweig, H.; Kollann, C.; Rais, D. *Angew. Chem., Int. Ed.* **2006**, *45*, 5254–5274.
- (12) Braunschweig, H.; Fernández, I.; Frenking, G.; Radacki, K.; Seeler, F. *Angew. Chem., Int. Ed.* **2007**, *46*, 5212–5214.
- (13) Timms, P. L. *Acc. Chem. Res.* **1973**, *6*, 118–123.
- (14) Pachaly, B.; West, R. *Angew. Chem.* **1984**, *96*, 444–445; *Angew. Chem. Int. Ed. Engl.* **1984**, *23*, 454–455.
- (15) Shimoi, M.; Ikubo, S.; Kawano, Y. *J. Am. Chem. Soc.* **1998**, *120*, 4222–4223.
- (16) Irvine, G. J.; Rickard, C. E. F.; Roper, W. R.; Williamson, A.; Wright, L. J. *Angew. Chem., Int. Ed.* **2000**, *39*, 948–950.
- (17) Cowley, A. H.; Lomeli, V.; Voigt, A. *J. Am. Chem. Soc.* **1998**, *120*, 6401–6402.
- (18) (a) Aldridge, S.; Coombs, D. L.; Jones, C. *Chem. Commun.* **2002**, 856–857. (b) Coombs, D. L.; Aldridge, S.; Jones, C.; Willock, D. J. *J. Am. Chem. Soc.* **2003**, *125*, 6356–6357. (c) Kays (nee Coombs), D. L.; Day, K. J.; Ooi, L.-L.; Aldridge, S. *Angew. Chem., Int. Ed.* **2005**, *44*, 7457–7460. (d) Aldridge, S.; Jones, C.; Gans-Eichler, T.; Stasch, A.; Kays (nee Coombs, D. L.; Coombs, N. D.; Willock, D. J. *Angew. Chem., Int. Ed.* **2006**, *45*, 6118–6122. (e) Vidovic, D.; Pierce, G. A.; Aldridge, S. *Chem. Commun.* **2009**, 1157–1171.
- (19) Braunschweig, H.; Colling, M.; Kollann, C.; Englert, U. *J. Chem. Soc., Dalton Trans.* **2002**, 2289–2296.
- (20) (a) Braunschweig, H.; Forster, M.; Radacki, K.; Seeler, F.; Whittell, G. R. *Angew. Chem., Int. Ed.* **2007**, *46*, 5212–5214. (b) Braunschweig, H.; Forster, M.; Kupfer, T.; Seeler, F. *Angew. Chem., Int. Ed.* **2008**, *47*, 5981–5983.
- (21) (a) Braunschweig, H.; Dewhurst, R. D.; Herbst, T.; Radacki, K. *Angew. Chem., Int. Ed.* **2008**, *47*, 5978–5980. (b) Apostolico, L.; Braunschweig, H.; Crawford, A. G.; Herbst, T.; Rais, D. *Chem. Commun.* **2008**, 497–498.

- (22) (a) Krogh-Jespersen, K.; Cremer, D.; Dill, J. D.; Pople, J. A.; Schleyer, P.; von, R. *J. Am. Chem. Soc.* **1981**, *103*, 2589–2594. (b) Eisch, J. J.; Shafii, B.; Odom, J. D.; Rheingold, A. L. *J. Am. Chem. Soc.* **1990**, *112*, 1847–1853.
- (23) Braunschweig, H.; Herbst, T.; Rais, D.; Seeler, F. *Angew. Chem. Int. Ed.* **2005**, *44*, 7461–7463.
- (24) (a) Habben, C.; Meller, A. *Chem. Ber.* **1984**, *117*, 2531–2537. (b) Brown, C.; Cragg, R. H.; Miller, T. J.; Smith, D. O. *J. Organomet. Chem.* **1983**, *244*, 209–215.

**Scheme 1.** (a) Thermolytic Borylene Transfer to Group 9 Cyclopentadienylmetallocarbonyls, (b) Formation of Half-Sandwich Vanadium Complex by Metal to Metal Borylene Transfer, and (c) Photolytic Borylene Transfer to Alkynes to Give Borirenes



[[ $(\mu\text{-BN}(\text{SiMe}_3)_2(\text{RC}=\text{C}^-))_2$ ]. (**5**: R = C<sub>6</sub>H<sub>5</sub> and **6**: R = C<sub>6</sub>H<sub>4</sub>-4-OMe). By employing diynes with adjacent triple bonds, that is 1,4-diphenylbuta-1,3-diyne and 1,4-bis(4-methoxyphenyl)buta-1,3-diyne, two bisborirenes, **5** and **6**, have been isolated in good yields upon photolysis with **1**. The presence of a <sup>11</sup>B{<sup>1</sup>H} resonance at  $\delta = 24.0$  ppm in each case is consistent with the proposed structure, while single <sup>1</sup>H NMR resonances for the SiMe<sub>3</sub> groups at  $\delta = 0.29$  (**5**) and 0.27 ppm (**6**) indicate highly symmetrical molecules in solution, and thus rapid rotation around the B–N bond at room temperature. On the basis of the NMR data combined with mass spectrometric analysis, **5** and **6** are formulated as [(BN(SiMe<sub>3</sub>)<sub>2</sub>(RCC))<sub>2</sub>] (**5**: R = C<sub>6</sub>H<sub>5</sub> and **6**: R = C<sub>6</sub>H<sub>4</sub>-4-OMe).

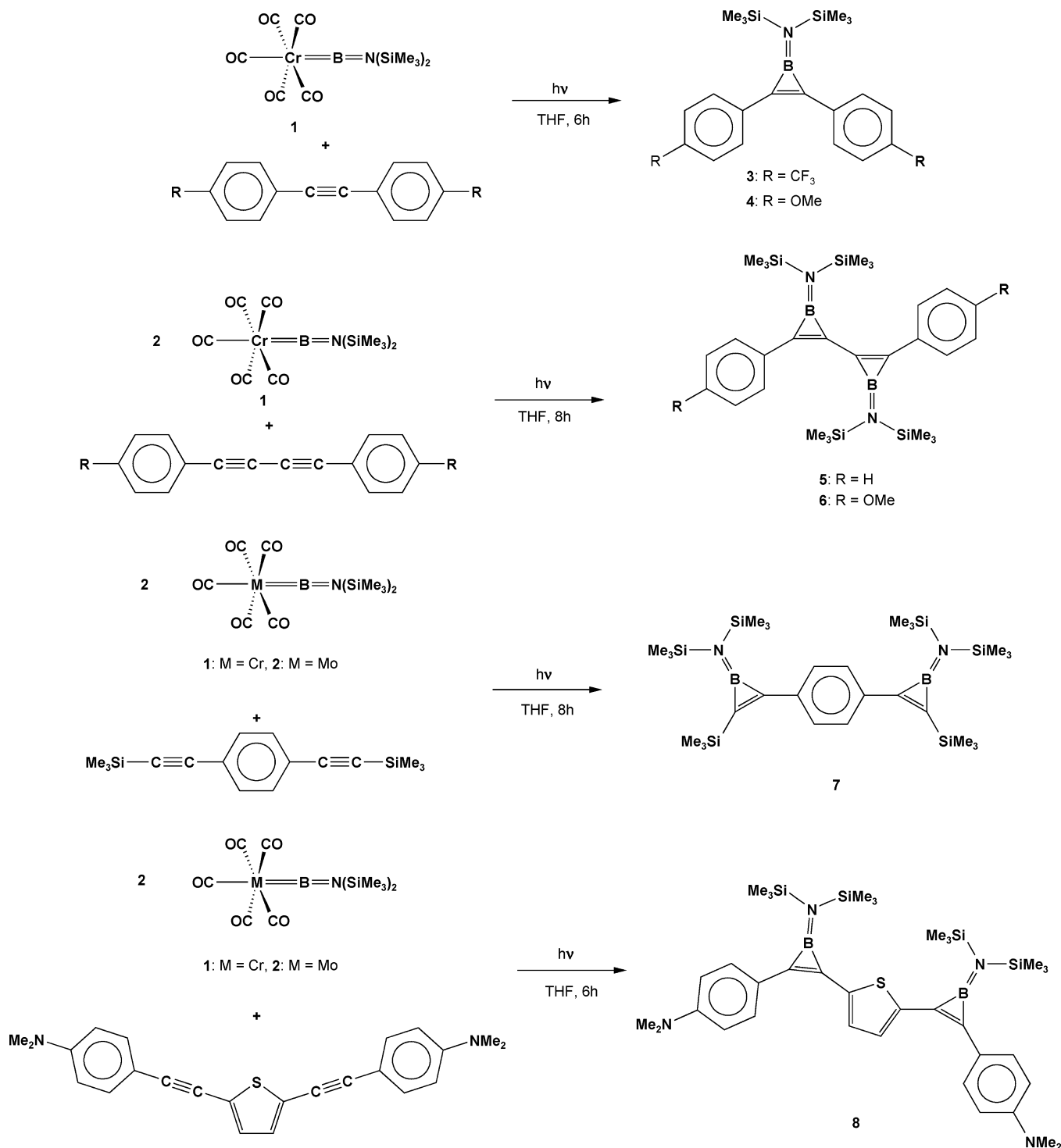
Single crystals suitable for X-ray diffraction analysis of **6** were obtained from a hexane solution at  $-60$  °C, thus allowing for the first structural characterization of a bisborirene (Figure 1). The molecule crystallizes in the space group  $P\bar{1}$  with  $Z = 2$  and is composed of two almost identical halves defined by the borirene rings and their *exo*-substituents, which are linked via the central C2–C3 bond; thus, an approximate C<sub>2</sub> symmetry is adopted. As indicated by a dihedral angle of 90.4°, the two boracyclopropene moieties are oriented almost perpendicular to each other, thus minimizing steric congestion imposed by the bulky N(SiMe<sub>3</sub>)<sub>2</sub> substituents. As the geometry of both borirene subunits is identical within the experimental error, only one set of data will be discussed. The distances within the BC<sub>2</sub> ring (C1–B1 = 1.482(2), B1–C2 = 1.500(2) and C1–C2

= 1.367(2) Å) are comparable to those of structurally characterized borirenes with boron-bound mesityl (B–C = 1.450(1) and 1.464(1), C–C = 1.380(9) Å),<sup>22b</sup> [( $\eta^5\text{-C}_5\text{Me}_5$ )(OC)<sub>2</sub>Fe]– (B–C = 1.490(4), C–C = 1.371(3) Å),<sup>12</sup> and amino substituents (B–C = 1.485(3), C–C = 1.376(4) Å).<sup>23</sup>

These structural findings have been interpreted as indicative of extensive delocalization of the two  $\pi$ -electrons over a three-center bonding molecular orbital comprised of the p<sub>z</sub>-atomic orbitals of boron and carbon.<sup>25</sup> In the case of **6**, this kind of delocalization is likely to be attenuated by the presence of the  $\pi$ -donating amino substituent. Indeed, a slightly elongated B–N separation of 1.417(2) Å, which matches that of the aforementioned aminoborirene (1.421(4) Å),<sup>23</sup> possibly indicates a weaker than normal  $\pi$  interaction between the boron and nitrogen centers as a result of the aromatic character of the boracyclopropene ring. Thus, there remains a question of the degree of B–N  $\pi$ -bonding vs aromaticity of the borirene ring, which will be addressed further by dynamic NMR spectroscopic studies and DFT calculations, *vide infra*. Finally, it should be mentioned that the central C2–C3 distance of 1.421(2) Å is significantly shorter than the central C–C single bond length of 1.483(1) Å in butadiene, linking two sp<sup>2</sup>-hybridized C-atoms,<sup>25</sup> but is comparable to the central C–C bond in [(Rh(PMe<sub>3</sub>)<sub>3</sub>(Cl))<sub>2</sub>( $\mu$ -(1,2- $\eta^2$ ):(3,4- $\eta^2$ )-4-F<sub>3</sub>C–C<sub>6</sub>H<sub>4</sub>–C≡C–C≡C–C<sub>6</sub>H<sub>4</sub>–4-CF<sub>3</sub>)]

(25) Marais, D. J.; Sheppard, N.; Stoicheff, B. P. *Tetrahedron* **1962**, 163–169.

**Scheme 2.** Synthesis of Mono- and Bis-bis-(trimethylsilyl)aminoborirenes, from Borylene Complexes,  $[(\text{CO})_5\text{M}=\text{B}=\text{N}(\text{SiMe}_3)_2]$  ( $\text{M} = \text{Cr}$  and  $\text{Mo}$ )



(1.405(4) Å), which connects the two conjugated  $\text{C}\equiv\text{C}$ -triple bonds each coordinated to one rhodium center.<sup>26</sup> We interpret this short  $\text{C}2-\text{C}3$  distance as indicative of a strong electronic interaction between the boracyclopropene rings. DFT calculations agree with the latter interpretation. The Wiberg bond order for the  $\text{C}2-\text{C}3$  bond order is  $>1$  for both bis-borirenes (1.10 for **5** and 1.09 for **6**). Moreover, the calculated hybridization of the carbon atoms  $\text{C}2/\text{C}3$  is  $sp^{1.57}$  in borirene **5** and  $sp^{1.56}$  in compound **6** which indicates a high degree of s-character in the  $\text{C}2-\text{C}3$  bonding orbitals at the carbon

atoms. The results thus confirm the strong electronic interaction which is responsible for the observed rather short  $\text{C}-\text{C}$  distances. The influence of lateral boryl groups on the electronic structure of  $\pi$ -conjugated oligomers and polymers has been reported by Jäkle et al. in bis(dimesitylboryl) substituted oligothiophenes and by Yamaguchi et al. in

(26) Ward, R. M.; Batsanov, A. S.; Howard, J. A. K.; Marder, T. B. *Inorg. Chim. Acta* **2006**, *359*, 3671–3676.

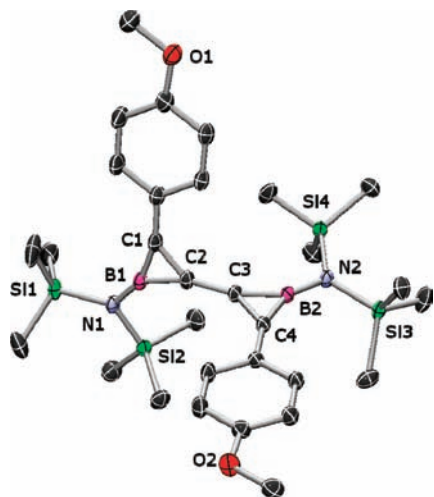


**Figure 1.** Molecular structure of **6**. Relevant bond lengths [Å] and angles [deg]: N1–B1 1.417(2), C1–B1 1.482(2), B1–C2 1.500(2), B2–N2 1.420(2), B2–C4 1.483(2), B2–C3 1.497(2), C2–C3 1.421(2), N1–Si1 1.758(1), Si1–C31 1.861(2), C1–C2 1.367(2), C3–C4 1.370(2), C1–B1–N1, 153.62(1), C1–B1–C2 54.59(8), N2–B2–C3 145.63(1), B1–N1–Si1 113.13(9), B2–N2–Si3 121.38(9), N1–Si1–C31 108.48(6). Ellipsoids drawn at the 50% probability level.

oligo(phenyleneethynylene)s (OPE's) containing bis(dimethylsilyl) functionalities.<sup>2d,e</sup>

[1,4-Bis- $\{(\mu\text{-BN}(\text{SiMe}_3)_2(\text{SiMe}_3\text{C}=\text{C}))\}_2\text{C}_6\text{H}_4$ ], **7** and [2,5-Bis- $\{(\mu\text{-BN}(\text{SiMe}_3)_2((\text{C}_6\text{H}_4\text{-4-NMe}_2)\text{C}=\text{C}))\}_2$ thiophene], **8**. In addition to the aforementioned alkynes and 1,3-diyne, a different type of substrate was employed, in which the two alkyne functionalities are separated by a conjugated spacer. Analogous to the preparation of **3–6**, photolysis of **1** with 1,4-bis(trimethylsilyl)ethynylbenzene and 2,5-bis(4-*N,N*-dimethylaminophenylethynyl)thiophene furnished aminoborirenes **7** and **8**, respectively, in good yield. Singlet  $^1\text{H}$  NMR resonances at  $\delta = 29.1$  (**7**) and 24.2 ppm (**8**) are in the expected range for borirene products. The mass spectrum of **7** is consistent with a formula containing two B, two N and six Si atoms and the parent ion mass of 612 corresponds to addition of two  $\text{BN}(\text{SiMe}_3)_2$  units to the dialkyne scaffold. Consistent with these observations is the presence of two singlets in the room temperature  $^1\text{H}$  NMR spectrum at  $\delta = 0.27$  and 0.34 ppm in a 1:2 ratio, which are associated with the carbon and nitrogen bound  $\text{SiMe}_3$ -groups, respectively. The observation of only one  $\text{N}(\text{SiMe}_3)_2$  resonance implies rapid rotation around the B–N bond at room temperature. However, the  $^1\text{H}$  NMR spectrum at  $-90^\circ\text{C}$  clearly shows two separate signals for the nitrogen-bound trimethylsilyl groups separated by 68 Hz. From 700 MHz VT  $^1\text{H}$  NMR spectroscopy, a value of  $\Delta G^\ddagger = 38.7$  kJ/mol at the coalescence temperature of  $-79^\circ\text{C}$  was computed for the rotational barrier, which is significantly smaller (by ca. 30 kJ/mol) than those commonly observed for B–N  $\pi$ -bonds.<sup>24</sup> Given the fact that there is an additional signal of equal intensity for the carbon-bound  $\text{SiMe}_3$  group close by, NOESY spectroscopy at  $-90^\circ\text{C}$  was used to confirm which pair of  $\text{SiMe}_3$  groups was exchanging. We also measured, as above, a similar barrier of 43.1 kJ/mol at the coalescence temperature of  $-68^\circ\text{C}$  for the related, previously reported<sup>23</sup> bis(borirene) [ $\{(\mu\text{-BN}(\text{SiMe}_3)_2(\text{Me}_3\text{SiC}=\text{C}))\}_2$ ] (**9**) formed via the transfer of two borirene groups to 1,4-bis(trimethylsilyl)buta-1,3-diyne. Via DFT calculations, we also computed the barrier to rotation about the B–N bond in the previously reported<sup>23</sup> symmetric borirene compound [ $(\mu\text{-BN}(\text{SiMe}_3)_2(\text{Me}_3\text{SiC}=\text{CSiMe}_3))$ ] (**10**) (Figure 2, top left) to be

7.4 kcal mol<sup>-1</sup> corresponding to 31.0 kJ mol<sup>-1</sup>, in good agreement with the measured barrier for **7**. These findings, together with the aforementioned structural data, lend further support to the description of the BN linkage in such aminoborirenes as a rather weak double bond, whose  $\pi$ -contribution is reduced by the incorporation of the  $p_z$ -orbital at boron into the  $2\pi$ -electron aromatic ring. Indeed, as shown in Figure 2 (top right), one observes only a small drop in the boron  $p_z$ -orbital occupancy from ca. 0.43 to ca. 0.37 electrons upon rotation to a dihedral angle between the  $\text{BNSi}_2$  and  $\text{BC}_2$  planes of  $90^\circ$ , indicative of the relatively small B–N  $\pi$ -component even at  $0^\circ$  dihedral.

In the case of **8**, spectroscopic data in addition to the aforementioned  $^{11}\text{B}$  NMR resonance clearly indicate the formation of a bisborirene. The NMR behavior of **8** is very similar indeed to that of **7**, differing most noticeably in small changes of proton shielding.  $^1\text{H}$  NMR spectrum of **8** shows singlets at  $\delta = 0.46$  for the four  $\text{SiMe}_3$  groups and at 7.64 ppm for the two protons in the thiophene ring. These data together with characteristic  $^{13}\text{C}$  NMR resonances at  $\delta = 3.6$  for the  $\text{SiCH}_3$  groups, and 130.4 ppm for the two CH groups in the thiophene ring, suggest rapid rotation around the B–N bond.

Crystals of **7**, were obtained by cooling a concentrated hexane solution to  $-60^\circ\text{C}$ . The single crystal X-ray diffraction structure of **7**, shown in Figure 3, confirms the structural inferences made on the basis of the spectroscopic data. The molecule crystallizes in the triclinic space group  $P\bar{1}$  with  $Z = 1$ , and thus lies on a crystallographic inversion center. The dihedral angles of  $56.21(3)^\circ$  between the spacer (phenyl) and the boracyclopentene units is considerably smaller than in **6** in which the rings are almost perpendicular to each other. This may be due to the presence of a phenyl ring which minimizes the steric overcrowding imposed by the bulky  $\text{N}(\text{SiMe}_3)_2$  groups. The overall geometry of the borirene rings in **7** resembles that of **6**, displaying B–C separations of 1.473(3) and 1.498(3) Å, and a C1–C2 distance of 1.362(3) Å. Interestingly, the carbon–carbon bond length of 1.470(3) Å, connecting the BCC and phenyl rings, falls between the corresponding C–C single bond distance observed in butadiene (1.483(1) Å)<sup>25</sup> and bisborirene **6** (1.421(2) Å). The bond length is similar to that of the C–C bond linking the phenyl group with the olefin in styrene derivatives, for example (disodium)1,4-bis(boratastyryl)benzene (1.464(4) Å).<sup>27</sup>

To analyze the bonding situations in the synthesized borirenes **3–8** in more detail we first carried out DFT calculations on the model compound  $(\text{H}_3\text{Si})_2\text{NBC}_2(\text{SiH}_3)_2$  (**10M**). The nature of the bonding interactions was investigated with the AIM (atoms in molecules)<sup>28</sup> method and with the EDA (energy decomposition analysis) partitioning procedure,<sup>29</sup> which has previously been used by us to investigate chemical bonds in other boron compounds.<sup>30</sup>

Figure 4 shows the contour line diagrams of the Laplacian distribution  $\nabla^2\rho(r)$  in the plane of the three-membered ring. The B–N bond in **10M** has an area of charge concentration ( $\nabla^2\rho(r) < 0$ , solid lines) at the nitrogen end, while the boron end carries

(27) Lee, B. Y.; Bazan, G., *Z. J. Am. Chem. Soc.* **2000**, *122*, 8577–8578.

(28) Bader, R. F. W. *Atoms in Molecules. A Quantum Theory*; Oxford University Press: Oxford, 1990.

(29) See Computational Details.

(30) (a) Uddin, J.; Frenking, G. *J. Am. Chem. Soc.* **2001**, *123*, 1683–1693. (b) Chen, Y.; Frenking, G. *J. Chem. Soc., Dalton Trans.* **2001**, 434–440. (c) Dörr, M.; Frenking, G. *Z. Anorg. Allg. Chem.* **2002**, *628*, 843–850. (d) Bessac, F.; Frenking, G. *Inorg. Chem.* **2003**, *42*, 7990–7994. (e) Erhardt, S.; Frenking, G. *Chem.–Eur. J.* **2006**, *12*, 4620–4629.

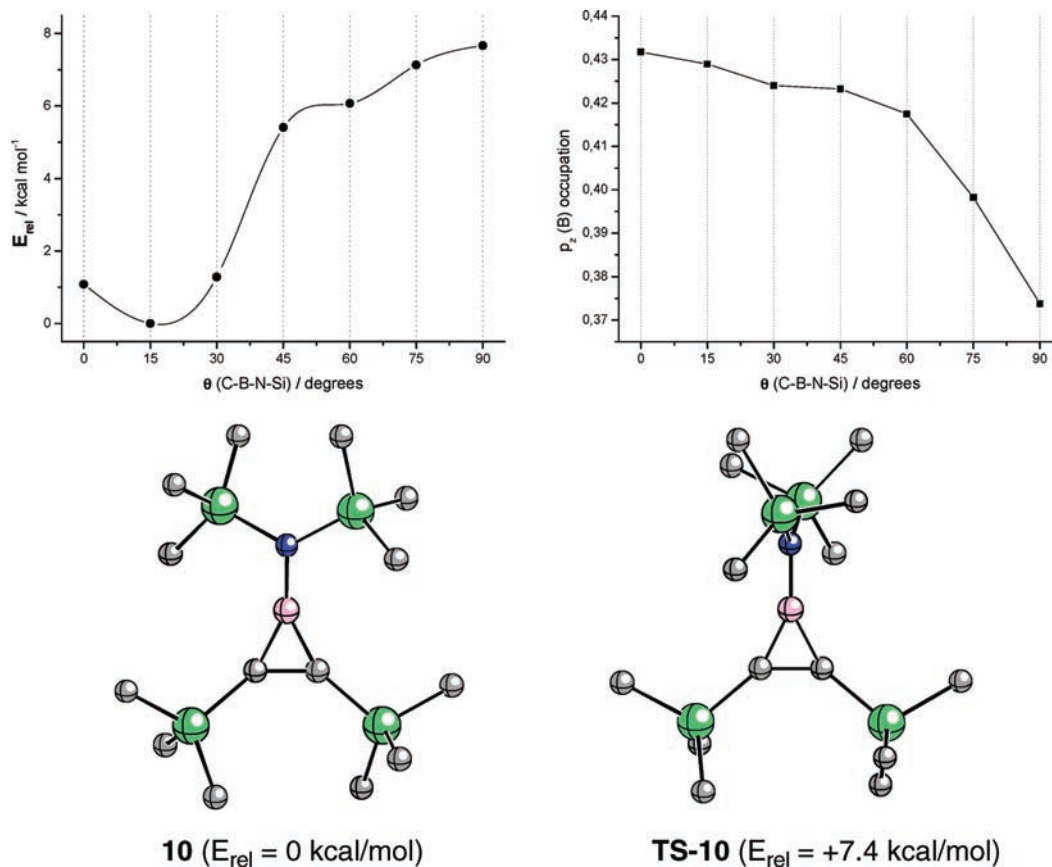


**Figure 2.** (Top) Relative energy of  $[(\mu\text{-BN}(\text{SiMe}_3)_2)(\text{Me}_3\text{SiC}=\text{CSiMe}_3)]$  (left) and boron  $p_z$  orbital occupation (right) as a function of the dihedral angle between the  $\text{BNSi}_2$  and  $\text{BC}_2$  planes. (Bottom) Ball and stick representations of the calculated structures at the energy minimum (left) and transition state for B–N bond rotation (right). Hydrogen atoms were omitted for clarity.

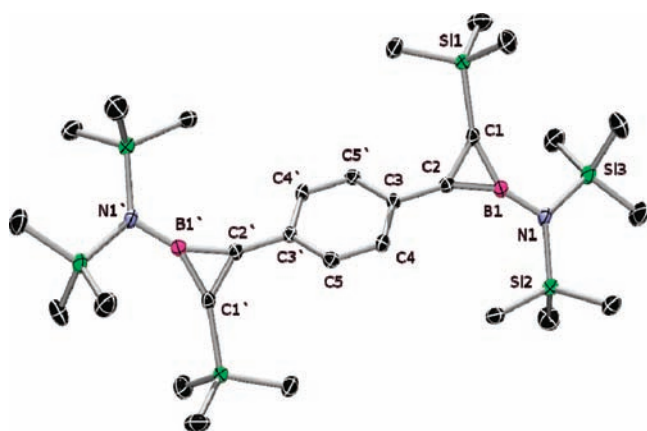


**Figure 3.** Molecular structure of **7**. Relevant bond lengths [ $\text{\AA}$ ] and angles [deg]: B1–N1 1.423(3), B1–C2 1.473(3), B1–C1 1.498(3), N1–Si2 1.751(2), C1–Si1 1.858(2), C2–C1 1.362(3), C2–C3 1.470(3), N1–B1–C2 154.95(2), N1–B1–C2 150.33(2), C2–B1–C1 54.59(1), B1–N1–Si2 120.35(1), B1–N1–Si3 113.90(1), C1–C2–C3 136.72(2), C1–C2–B1 63.63(2), C3–C2–B1 159.48(2). Ellipsoids drawn at the 50% probability level.

an area of charge depletion ( $\nabla^2\rho(r) > 0$ , dashed lines) which is typical for a polar electron-sharing bond.<sup>28,31</sup> As expected, **10M** is characterized by the AIM method as three-membered cyclic species possessing two B–C and one C–C bond paths and one  $\text{BC}_2$  ring critical point.

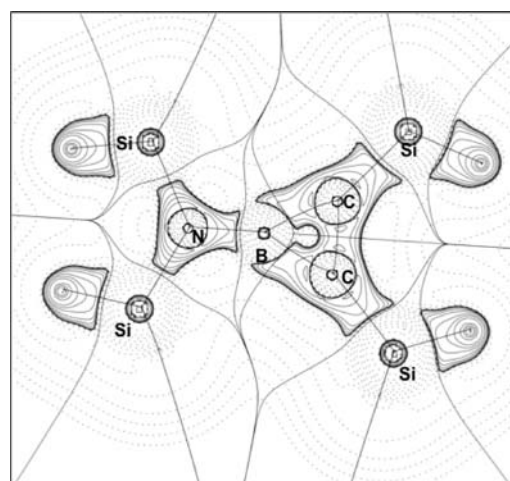


**Figure 4.** Contour line diagrams  $\nabla^2\rho(r)$  of **10M** in the  $\text{BC}_2$  ring plane. Solid lines indicate areas of charge concentration ( $\nabla^2\rho(r) < 0$ ) while dashed lines show areas of charge depletion ( $\nabla^2\rho(r) > 0$ ). The solid lines connecting the atomic nuclei are the bond paths. The solid lines separating the atomic basins indicate the zero-flux surfaces crossing the molecular plane.

More detailed information about the boron bonds is given by the EDA results which are summarized in Table 1.

The B–N electron-sharing bond in **10M** was analyzed using the fragments  $(\text{H}_3\text{Si})_2\text{N}$  and  $\text{BC}_2(\text{SiH}_3)_2$  in the electronic doublet state. The EDA indicates that the attractive B–N interactions in **10M** mainly result from orbital (covalent) interactions (59.8%), rather than from electrostatic attraction (40.2%). The most interesting EDA data come from the breakdown of the

(31) Frenking, G.; Koch, W.; Gauss, J.; Cremer, D.; Sawaryn, A.; Schleyer, P. v. R. *J. Am. Chem. Soc.* **1986**, *108*, 5732–5740.

**Table 1.** Results of the EDA at BP86/TZ2P (Energy Values in kcal/mol)

$\Delta E_{\text{int}}$	-142.9	-213.8	-150.4	-250.3
$\Delta E_{\text{Pauli}}$	305.6	408.0	327.5	353.1
$\Delta E_{\text{elstat}}^{[a]}$	-180.5 (40.2%)	-245.6 (39.5%)	-198.0 (41.4%)	-271.8 (45.0%)
$\Delta E_{\text{orb}}^{[a]}$	-268.0 (59.8%)	-376.2 (60.5%)	-279.8 (58.6%)	-331.7 (55.0%)
$\Delta E_{\sigma}^{[b]}$	-246.3 (91.9%)	-345.7 (91.8%)	-255.2 (91.2%)	-318.9 (96.1%)
$\Delta E_{\pi}^{[b]}$	-21.8 (8.1%)	-30.6 (8.1%)	-24.6 (8.8%)	-12.8 (3.9%)
$\Delta E_{\text{prep}}$	18.0		27.7	
$\Delta E (=D_e)$	-124.9		-122.7	
$r(X-X) / \text{\AA}$	B-N:1.423	C-C:1.379	B-N:1.451	B-C:1.592
Fragments	NSi <sub>2</sub> H <sub>6</sub> (d) BC <sub>2</sub> Si <sub>2</sub> H <sub>6</sub> (d)	H <sub>6</sub> Si <sub>2</sub> NB(t) C <sub>2</sub> Si <sub>2</sub> H <sub>6</sub> (t)	NSi <sub>2</sub> H <sub>6</sub> (d) BC <sub>2</sub> H <sub>6</sub> (d)	H <sub>6</sub> Si <sub>2</sub> NB(t) C <sub>2</sub> H <sub>6</sub> (t)

<sup>a</sup> Percentage values in parentheses give the contribution to the total attractive interactions  $\Delta E_{\text{elstat}} + \Delta E_{\text{orb}}$ . <sup>b</sup> Percentage values in parentheses give the contribution to the total orbital interactions  $\Delta E_{\text{orb}}$ .

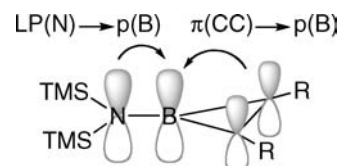
orbital term  $\Delta E_{\text{orb}}$  into  $\sigma$  and  $\pi$  contributions which clearly indicates that the B–N linkage is indeed a rather weak double bond. The  $\Delta E_{\pi}$  term contributes only 8.1% (–21.8 kcal/mol) to the total orbital interactions. Interestingly, this  $\pi$ -contribution is reduced by the incorporation of the  $p_z$ -orbital at boron into the  $2\pi$ -electron aromatic ring in **10M** compared to (H<sub>3</sub>Si)<sub>2</sub>NB(CH<sub>3</sub>)<sub>2</sub> (**11**). The EDA data clearly shows an increase in the  $\Delta E_{\pi}$  term in **11** which lacks the contribution of the three-membered ring. Table 1 also gives the EDA results for the B–C<sub>2</sub>(SiH<sub>3</sub>)<sub>2</sub> bonds in **10M** using the interacting fragments in the triplet state. The breakdown of  $\Delta E_{\text{int}}$  into the attractive and repulsive interactions reveals that the main contribution to the total interaction energy comes from the orbital term  $\Delta E_{\text{orb}}$  (60.5%). The most interesting information is derived from the calculated values for the B–C<sub>2</sub>(SiH<sub>3</sub>)<sub>2</sub>  $\pi$ -interactions in the three-membered ring. The  $\Delta E_{\text{orb}}(\pi)$  value in the parent borirene **10M** is –30.6 kcal/mol, indicating substantial cyclic delocalization which suggests some aromatic character of the ring. The aromaticity is supported by the computed NICS(0) and NICS(1) values, –15.3 and –12.9 ppm respectively.<sup>32</sup> This means that the boron atom in **10M** has a stronger  $\pi$ -interaction with the C=C  $\pi$  electrons than with the (SiH<sub>3</sub>)<sub>2</sub>N lone pair. The lack of a C=C double bond in **11** leads to a rather small  $\Delta E_{\text{orb}}(\pi)$  contribution (–12.8 kcal/mol) which is even smaller than the value for the  $\pi$ -interaction in the B–N bond.

Similar conclusions can be drawn using the second order perturbation energies from the NBO method. As readily seen in Table 2 the two-electron stabilizing donation from the  $\pi(\text{C}=\text{C})$  molecular orbital to the  $p_z$ -atomic orbital at boron in borirene **10** is substantially higher (associated second order energy,  $\Delta E^{(2)} = -93.8$  kcal/mol) than the corresponding electronic donation from the nitrogen atom lone pair ( $\Delta E^{(2)} = -46.9$  kcal/mol, Table 2). These data are in nice agreement with the EDA results and therefore we shall use the computed NBO-data to explain the changes in the strength of the  $\pi(\text{C}=\text{C})$

**Table 2.** Computed Second Order Perturbation Energies (in kcal/mol)<sup>a</sup> Associated with the Two-Electron Donations to the  $p_z$ -Atomic Orbital at the Boron Atom (see Figure 5) in Compounds **3–8** and **10**

compound	LP(N) → p(B)	$\pi(\text{C}=\text{C}) \rightarrow p(\text{B})$
<b>10</b>	–46.9	–93.8
<b>3</b>	–45.7	–94.2
<b>4</b>	–43.5	–100.6
<b>5</b>	–65.7	–99.1
<b>6</b>	–64.3	–100.7
<b>7</b>	–61.2	–94.2
<b>8</b>	–52.3	–101.2

<sup>a</sup> All values have been computed at the B3LYP/def2-SVP level.

**Figure 5.** Schematic representation of the two-electron stabilizing donation to the  $p$ -atomic orbital at boron atom in borirenes **3–10**.

or nitrogen lone pair to  $p_z$ -(boron) donation in the borirenes **3–8** (Figure 5).

Table 2 shows that the replacement of the trimethylsilyl groups in **10** by a  $p$ -methoxyphenyl substituent in **4** yields a small increase in the  $\pi(\text{C}=\text{C}) \rightarrow p_z(\text{B})$  donation due to the presence of the  $\pi$ -donor methoxy groups and a slight decrease of the LP(N) →  $p_z(\text{B})$  donation. However, the presence of the weak  $\pi$ -acceptor groups CF<sub>3</sub> in **3** does not lead to an expected decrease of the  $\pi(\text{C}=\text{C}) \rightarrow p_z(\text{B})$  donation which remains practically the same. This means that the electronic effect exerted by the trifluoromethylphenyl substituent in borirene **3** is comparable to the trimethylsilyl group in **10**. Strikingly, the presence of a second borirene moiety in compounds **5–8** compared to **10** yields in all cases a clear enhancement of the LP(N) →  $p_z(\text{B})$  donation which is a consequence of the extended  $\pi$ -conjugation. This effect is nicely reflected in the shortening of the B–N bond length (see Figure 6). In the latter *bis*-borirenes the  $\pi(\text{C}=\text{C}) \rightarrow p_z(\text{B})$  donation remains higher than the LP(N) →  $p_z(\text{B})$  donation which is comparable to the value in **4** due to the presence of the phenyl groups attached to the C=C linkage.

(32) NICS(0) value was computed at the (3,+1) ring critical point of the electron density due to its high sensitivity to diamagnetic effects and its unambiguous character. See: (a) Fernández, I.; Sierra, M. A.; Cossío, F. P. *J. Org. Chem.* **2006**, *71*, 6178. (b) Fernández, I.; Cossío, F. P.; Sierra, M. A. *J. Org. Chem.* **2007**, *72*, 1488. (c) Fernández, I.; Sierra, M. A.; Cossío, F. P. *J. Org. Chem.* **2008**, *73*, 2083, and references therein.

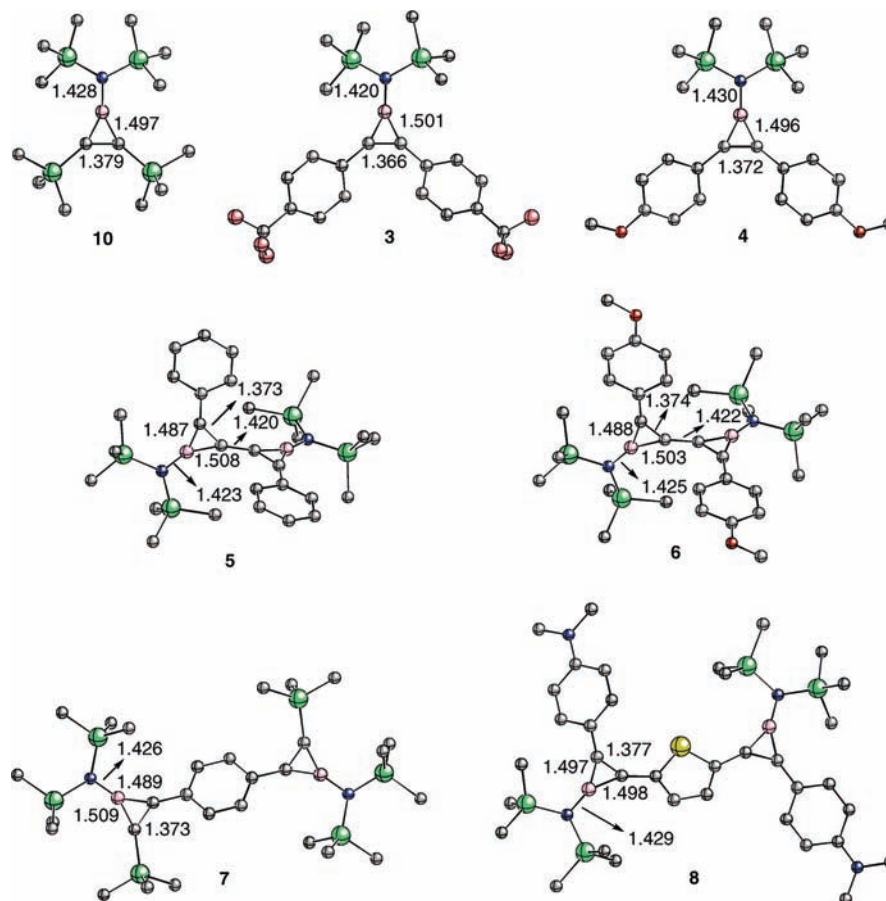


**Figure 6.** Optimized geometries of borirenes 3–10. Hydrogen atoms were omitted for clarity.

Finally, the presence of a  $\pi$ -spacer connecting both borirene moieties in compounds **7** and **8** also enhances the donation from the nitrogen atom lone pair to the boron atom thus confirming the extended  $\pi$ -conjugation in these species. As expected, the  $\pi(\text{C}=\text{C}) \rightarrow p_z(\text{B})$  donation is higher in **8** due to the attachment of the  $\pi$ -donor 4-*N*-dimethylphenyl substituent to the borirene ring compared to the TMS group in **7**.

UV–vis spectra of the borirene compounds were recorded in either  $\text{CH}_2\text{Cl}_2$  or hexane solutions. In contrast to the spectra of the corresponding alkyne or diyne precursors, which show sharp absorptions featuring well-defined vibrational fine structure, most likely arising from the  $\text{C}\equiv\text{C}$  triple bonds, those of the borirenes display broad, featureless absorptions with maxima occurring at higher energies (Table 3). TD-DFT calculations in the gas phase (Table 3) give computed oscillator strengths which are in general accord with (i.e., generally follow the same trend) the experimental values of the extinction coefficients, with the notable exception of compound **8**, for which the observed low energy absorption is especially broad and thus the extinction coefficient is likely not a good measure of oscillator strength. There is also reasonable agreement of the TD-DFT computed lowest energy transition wavelengths with those measured in solution (i.e., within ca. 13–33 nm), with the exception of compounds **7** and **8**, which feature more extended conjugation paths between the two borirene moieties. In these latter cases, the computed values are significantly red-shifted from the measured ones, most likely a result of the fact that the computed values are based on optimized geometries which are relatively planar, maximizing conjugation. However, the rotational barriers around the C–C bonds linking the borirene moieties with the

**Table 3.** UV-Vis Absorption Spectra and TD-DFT Computed Transitions for the Borirene Compounds

compound	transition <sup>a</sup>	f, oscillator strength, <sup>a</sup> ( $\epsilon$ ) <sup>b</sup>	$\lambda$ /nm <sup>b</sup>	weight <sup>a</sup>
<b>3</b>	HOMO→LUMO	0.346 (12,200) <sup>c</sup>	302 (269) <sup>c</sup>	0.616
	HOMO-1→LUMO	0.567	309	0.183
<b>4</b>	HOMO→LUMO	(37,400) <sup>c</sup>	(279) <sup>c</sup>	0.634
	HOMO-1→LUMO	0.448 (24,200) <sup>d</sup>	280 (257) <sup>d</sup>	0.494
<b>5</b>	HOMO-1→LUMO+1	0.227	272	0.510
	HOMO-1→LUMO	0.763	283	0.479
	HOMO→LUMO+1	(34,600) <sup>c</sup>	(266) <sup>c</sup>	0.448
	HOMO-2→LUMO	0.424	272	0.133
<b>6</b>	HOMO-1→LUMO+1			0.484
	HOMO→LUMO			0.393
	HOMO-1→LUMO	0.256	330	0.229
	HOMO-1→LUMO+2	(16,800) <sup>d</sup>	(262) <sup>d</sup>	0.110
<b>7</b>	HOMO→LUMO			0.549
	HOMO-2→LUMO	0.426	298	0.507
	HOMO→LUMO			0.356
	HOMO→LUMO	0.935 (8,900) <sup>c</sup>	434 (387) <sup>c</sup>	0.668
<b>8</b>	HOMO-1→LUMO+2	0.461	267	0.124
	HOMO-1→LUMO+3	(13,100) <sup>c</sup>	(276) <sup>c</sup>	0.135
	HOMO-1→LUMO+4			0.461
	HOMO-1→LUMO	0.0031	326	0.104
<b>10</b>	HOMO→LUMO	(487) <sup>d</sup>	(313) <sup>d</sup>	0.680

<sup>a</sup> TD-DFT data calculated at the B3LYP/def2-SVP level.

<sup>b</sup> Experimental values in parentheses. <sup>c</sup> Recorded in  $\text{CH}_2\text{Cl}_2$ . <sup>d</sup> Recorded in *n*-hexane.

central phenylene or thienyl groups are likely to be relatively small, giving rise to free rotation in solution and thus, all rotamers will likely be populated at room temperature. As a result, the observed solution spectra contain Franck–Condon transitions arising from this ensemble of rotamers including



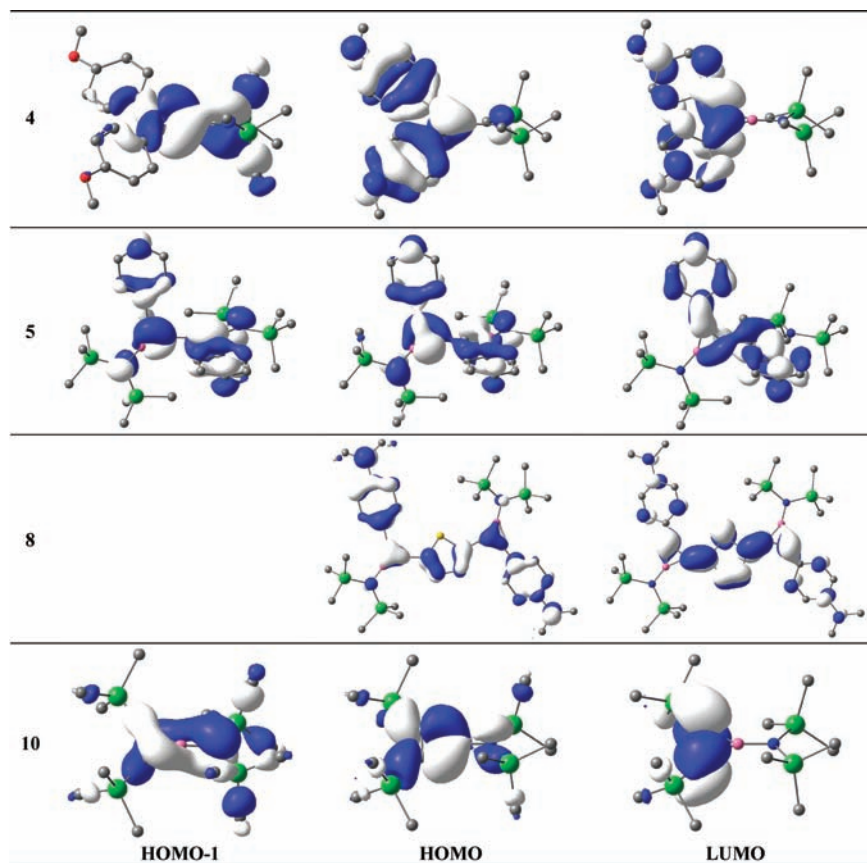


**Figure 7.** Molecular orbitals of compounds **4**, **5**, **8**, and **10** calculated at B3LYP/def2-SVP level (isosurface value of 0.035). Hydrogen atoms were omitted for clarity. See Figure 2 caption for additional details.

not only the highly conjugated planar conformations, but also twisted rotamers for which the conjugation length is greatly decreased. Compound **8** displays a strong, broad emission ( $\lambda_{\text{max}} = 463$  nm) in  $\text{CH}_2\text{Cl}_2$  solution, red-shifted compared with that seen for its precursor, 2,5-bis(4-*N,N*-dimethylamino-phenylethynyl)-thiophene, which occurs at 434 nm.<sup>33</sup> It is not unreasonable to assume that for **8**, the emission maximum is closely related to the 0,0 transition energy,<sup>33</sup> and is thus a more reasonable value to compare with the TD-DFT computed value, with which it is in much closer agreement, again, bearing in mind that the latter is a gas-phase value whereas the former was recorded in a moderately polar solvent. The large Stokes shift observed for this compound also supports the above reasoning. Key frontier orbitals involved in the optical transitions for several of the compounds are illustrated in Figure 7.

## Conclusion

The present article describes a facile synthetic method for a borylene based functionalization of organic substrates for which a variety of reagents of the type  $\text{R}-\text{C}\equiv\text{C}-\text{R}$  and  $\text{R}-\text{C}\equiv\text{C}-(\text{spacer})-\text{C}\equiv\text{C}-\text{R}$  were employed in stoichiometric amounts. This high yield synthetic procedure for the generation of borirenes not only confirmed the function of complexes **1–2** as valuable borylene sources, but also proved to be general with respect to the variety of alkynes that undergo the transformation. The bisborirenes, **6** and **7**, reported here are the first structurally

characterized bisborirenes and have an extended  $\pi$ -conjugation incorporating three-coordinate boron centers. The joint computational-experimental study presented here supports the view of the B–N linkage in these borirenes as a rather weak double bond whose  $\pi$ -contribution is reduced by the incorporation of the empty  $p_z$ -orbital at boron into the  $2\pi$ -electron aromatic ring.

## Experimental Section

**General.** All manipulations were performed either under dry argon or *in vacuo* using standard Schlenk line and glovebox techniques. Solvents (THF, ether, toluene and hexane) were purified by distillation under dry argon from sodium and stored under the same inert gas over molecular sieves. NMR spectra were acquired on Varian VNMRS-700 ( $^1\text{H}$ : 699.74;  $^{29}\text{Si}$ : 139.02 MHz), Varian Unity 500 ( $^1\text{H}$ : 499.834;  $^{11}\text{B}$ : 160.364;  $^{13}\text{C}$ : 125.697 MHz) or Bruker Avance 500 ( $^1\text{H}$ : 500.133;  $^{11}\text{B}$ : 160.472;  $^{13}\text{C}$ : 125.777 MHz) NMR spectrometers.  $^1\text{H}$  and  $^{13}\text{C}\{^1\text{H}\}$  NMR spectra were referenced to external TMS via the residual protio solvent ( $^1\text{H}$ ) or the solvent itself ( $^{13}\text{C}$ ).  $^{11}\text{B}\{^1\text{H}\}$  and  $^{29}\text{Si}\{^1\text{H}\}$  NMR spectra were referenced to external  $\text{BF}_3\cdot\text{OEt}_2$  and TMS, respectively. NMR probe temperatures were calibrated using a MeOH standard for VT NMR spectroscopic studies. UV–vis and fluorescence spectra were recorded in toluene if not otherwise indicated. UV–vis absorption spectra and extinction coefficients were obtained on a Hewlett-Packard 8453 diode array and a Shimadzu 1240 mini spectrophotometer using standard 1 cm width quartz cells. Fluorescence spectra were recorded at right angles to the excitation source on dilute solutions using a Horiba Jobin Yvon Fluoromax 3 spectrophotometer. The emission spectra were fully corrected using the manufacturer's correction curves for the spectral response of the emission optical components.

(33) Siddle, J. S.; Ward, R. M.; Collings, J. C.; Rutter, S. R.; Porrès, L.; Applegarth, L.; Beeby, A.; Batsanov, A. S.; Thompson, A. L.; Howard, J. A. K.; Boucekine, A.; Costuas, K.; Halet, J.-F.; Marder, T. B. *New J. Chem.* **2007**, *31*, 841–851.

Microanalyses were performed on either a Carlo Erba model 1106 or a Leco CHNS-932 Elemental Analyzer.  $\text{Na}_2[\text{M}(\text{CO})_5]^{34}$  ( $\text{M} = \text{Cr}$ , and  $\text{Mo}$ ), and  $\text{Cl}_2\text{B}(\text{SiMe}_3)_2^{35}$  were prepared according to the literature. Borylene complexes,  $(\text{OC})_5\text{M}=\text{BN}(\text{SiMe}_3)_2$  (**1**:  $\text{Cr}$  and **2**:  $\text{Mo}$ ),<sup>7</sup> 2,5-bis(4-*N,N*-dimethylamino-phenylethynyl)thiophene,<sup>33</sup> alkynes and diynes<sup>36</sup> were synthesized as reported in the literature. NMR spectroscopic experiments were performed in quartz NMR tubes. The light source was a Hg/Xe arc lamp (400–550 W) equipped with IR filters, irradiating at 210–600 nm. Large-scale experiments were performed in a 150-mL Schlenk flask equipped with a quartz cooling jacket into which a Hg lamp (125 W) was inserted vertically.

**Synthesis of Mono- and 1-Bis(trimethylsilyl)aminoborirenes, 3–8.** Compound **3**: In a 5 mm quartz NMR tube, a pale yellow solution of **1** (125 mg, 0.34 mmol) and 1,2-bis(4-(trifluoromethyl)phenyl)ethyne (104 mg, 0.33 mmol) in 1.5 mL of THF was irradiated for 5 h at room temperature. The volatile components were removed *in vacuo*, and the brown residue was extracted with 5 mL of hexane followed by centrifugation. The brown hexane solution was decanted from the brown residue and stored at  $-60^\circ\text{C}$  overnight to separate  $\text{Cr}(\text{CO})_6$ . After filtration, the solvent was removed *in vacuo* and **3** was isolated as an analytically pure yellow solid (0.11 g, 72% yield).  $^1\text{H}$  NMR:  $\delta = 7.30$  (m, 4H, *CH-m* or *CH-o* of  $\text{C}_6\text{H}_4$ ), 7.24 (m, 4H, *CH-m* or *CH-o* of  $\text{C}_6\text{H}_4$ ), 0.31 (s, 18H,  $\text{Si}(\text{CH}_3)_3$ );  $^{13}\text{C}\{^1\text{H}\}$ -NMR:  $\delta = 161.4$  (bs, C bonded to boron), 137.6 (s, *CH-m* of  $\text{C}_6\text{H}_4\text{-CF}_3$ ), 130.3 (q,  $^2J_{\text{C-F}} = 33$  Hz, C- $\text{CF}_3$ ), 125.9 (q,  $^3J_{\text{C-F}} = 4$  Hz, *CH-o* of  $\text{CF}_3$ ), 124.8 (q,  $^1J_{\text{C-F}} = 271$  Hz,  $\text{CF}_3$ ), 3.1 (s,  $\text{Si}(\text{CH}_3)_3$ );  $^{11}\text{B}\{^1\text{H}\}$ -NMR:  $\delta = 23.7$  (s). EI-MS  $m/z = 485$  ( $\text{M}^+$ ), 98 ( $\text{B}=\text{N}-\text{SiMe}_3^+$ ). Elemental analysis calcd. [%] for  $\text{C}_{22}\text{H}_{26}\text{Si}_2\text{BNF}_6$ : C 54.43, H 5.40, N 2.89; found: C 54.32, H 5.45, N 2.83.

**Compound 4.** In a 5 mm quartz NMR tube, a pale-yellow solution of **1** (110 mg, 0.30 mmol) and 1,2-bis(4-methoxyphenyl)ethyne (73 mg, 0.30 mmol) in 1.5 mL of THF was irradiated for 5 h at room temperature. The volatile components were removed *in vacuo*, and the brown residue was extracted with 8 mL of hexane followed by centrifugation. The brown hexane solution was decanted from the black residue and stored at  $-60^\circ\text{C}$  overnight to separate  $\text{Cr}(\text{CO})_6$ . After filtration, the solvent was removed *in vacuo* and **4** was isolated as an analytically pure yellow solid (90.4 mg, 74% yield).  $^1\text{H}$  NMR:  $\delta = 7.72$  (m, 4H, *CH-m* of  $\text{C}_6\text{H}_4\text{-OCH}_3$ ), 6.77 (m, 4H, *CH-o* of  $\text{C}_6\text{H}_4\text{-OCH}_3$ ), 3.28 (s, 6H,  $\text{OCH}_3$ ), 0.42 (s, 18H,  $\text{Si}(\text{CH}_3)_3$ );  $^{13}\text{C}\{^1\text{H}\}$ -NMR:  $\delta = 160.2$  (s, C- $\text{OCH}_3$ ), 157.7 (bs, C bonded to boron), 130.9 (s, *CH-m* of  $\text{C}_6\text{H}_4$ ), 126.9 (s, *C-i* of  $\text{C}_6\text{H}_4$ ), 114.6 (s, *CH-o* of  $\text{C}_6\text{H}_4$ ), 54.8 (s,  $\text{OCH}_3$ ), 3.4 (s,  $\text{Si}(\text{CH}_3)_3$ );  $^{11}\text{B}\{^1\text{H}\}$ -NMR:  $\delta = 24.8$  (s). EI-MS  $m/z = 409$  ( $\text{M}^+$ ). Elemental analysis calcd. [%] for  $\text{C}_{22}\text{H}_{32}\text{Si}_2\text{BNO}_2$ : C 64.53, H 7.88, N 3.42; found: C 64.50, H 7.62, N 3.42.

**Compound 5.** In a 5 mm quartz NMR tube, a pale-yellow solution of **1** (100 mg, 0.25 mmol) and 1,4-diphenylbuta-1,3-diyne (25 mg, 0.13 mmol) in 0.5 mL of *d*<sub>6</sub>-benzene was irradiated for 6 h at room temperature. The volatile components were removed *in vacuo*, and the brown residue was extracted with hexane (2 × 3 mL) followed by filtration using glass fiber. The filtrate was evaporated to dryness to afford an analytically pure yellow oil of **5** (63.7 mg, 90%).  $^1\text{H}$  NMR:  $\delta = 7.83$  (m, 4H, *CH-o* of  $\text{C}_6\text{H}_5$ ), 7.09 (m, 6H, *CH-m* and *CH-p* of  $\text{C}_6\text{H}_5$ ), 0.35 (s, 36H,  $\text{Si}(\text{CH}_3)_3$ );  $^{13}\text{C}\{^1\text{H}\}$ -NMR:  $\delta =$  (C bonded to boron not detected), 132.8 (s, *C-i* of  $\text{C}_6\text{H}_5$ ), 130.4 (s, *CH-m* or *CH-o*), 129.1 (s, *CH-m* or *CH-o*), 128.6 (s, *CH-p*), 3.2 (s,  $\text{Si}(\text{CH}_3)_3$ );  $^{11}\text{B}\{^1\text{H}\}$ -NMR:  $\delta = 24.0$  (s). EI-MS  $m/z = 544$  ( $\text{M}^+$ ). Elemental analysis calcd. [%] for  $\text{C}_{28}\text{H}_{46}\text{Si}_2\text{BN}_2$ : C 61.75, H 8.51, N 5.14; found: C 61.43, H 8.70, N 4.50.

**Compound 6.** In a 5 mm quartz NMR tube, a pale-yellow solution of **1** (100 mg, 0.25 mmol) and 1,4-bis(4-methoxyphenyl)buta-1,3-diyne (35.9 mg, 0.14 mmol) in 1 mL of THF was irradiated for 8 h at room temperature. The volatile components were removed *in vacuo*, and the brown residue was extracted with hexane (2 × 3 mL) followed by filtration through a pad of silica gel. The filtrate was stored at  $-30^\circ\text{C}$  for 2 weeks to afford yellow crystals of **6** (54.7 mg, 68%).  $^1\text{H}$  NMR:  $\delta = 7.81$  (m, 4H, *CH-m* of  $\text{C}_6\text{H}_4\text{-OCH}_3$ ), 6.63 (m, 4H, *CH-o* of  $\text{C}_6\text{H}_4\text{-OCH}_3$ ), 3.17 (s, 6H,  $\text{O-CH}_3$ ), 0.40 (s, 36H,  $\text{Si}(\text{CH}_3)_3$ );  $^{13}\text{C}\{^1\text{H}\}$ -NMR:  $\delta = 160.7$  (s, C- $\text{OCH}_3$ ), 149.4 (bs, C bonded to boron), 142.3 (bs, C bonded to boron), 132.2 (s, *CH-m* of  $\text{C}_6\text{H}_4$ ), 125.6 (s, *C-i* of  $\text{C}_6\text{H}_4$ ), 114.5 (s, *CH-o* of  $\text{C}_6\text{H}_4$ ), 54.7 (s,  $\text{OCH}_3$ ), 3.26 (s,  $\text{Si}(\text{CH}_3)_3$ );  $^{11}\text{B}\{^1\text{H}\}$ -NMR:  $\delta = 24.0$  (s). EI-MS  $m/z = 604$  ( $\text{M}^+$ ), 73 ( $\text{M} - \text{SiMe}_3^+$ ). Elemental analysis calcd. [%] for  $\text{C}_{30}\text{H}_{50}\text{Si}_4\text{B}_2\text{N}_2\text{O}_2$ : C 59.59, H 8.33, N 4.63; found: C 59.73, H 8.41, N 4.38.

**Compound 7.** In a 150 mL quartz Schlenk flask, a pale-yellow solution of **1** (350 mg, 0.96 mmol) or **2** (391 mg, 0.96 mmol) and 1,4-bis(trimethylsilyl)ethynylbenzene (131 mg, 0.48 mmol) in 15 mL of THF was irradiated for 4 h at room temperature. The volatile components were removed *in vacuo*, and the black residue was extracted with 10 mL of hexane followed by filtration using glass-fiber filter paper. The filtrate was stored at  $-30^\circ\text{C}$  overnight to remove a brown unknown solid as well as  $\text{Cr}(\text{CO})_6$ . After removing the residue the mother liquor was kept at  $-60^\circ\text{C}$  to afford colorless crystalline **7** (232 mg, 79%).  $^1\text{H}$  NMR:  $\delta = 7.53$  (s, 4H, of  $\text{C}_6\text{H}_4$ ), 0.34 (s, 36H,  $\text{N}(\text{Si}(\text{CH}_3)_3)_2$ ), 0.27 (s, 18H,  $\text{Si}(\text{CH}_3)_3$ );  $^{13}\text{C}\{^1\text{H}\}$ -NMR:  $\delta = 184.0$  (s, =C- $\text{SiMe}_3$ ), 172.8 (s, =C- $\text{C}_6\text{H}_4$ ), 137.4 (s, *C-i* of  $\text{C}_6\text{H}_4$ ), 127.5 (s, CH of  $\text{C}_6\text{H}_4$ ), 3.3 (s,  $\text{N-Si}(\text{CH}_3)_3$ ), 0.2 (s, =C- $\text{SiCH}_3$ );  $^{11}\text{B}\{^1\text{H}\}$ -NMR:  $\delta = 29.1$  (s).  $^{29}\text{Si}\{^1\text{H}\}$ -NMR:  $\delta = 5.95$  (s,  $\text{N-Si}(\text{Me}_3)_2$ ),  $-14.92$  (s, =C- $\text{SiMe}_3$ ). EI-MS  $m/z = 612$  ( $\text{M}^+$ ), 98 ( $\text{B}=\text{N}-\text{SiMe}_3^+$ ). Elemental analysis calcd. [%] for  $\text{C}_{28}\text{H}_{58}\text{Si}_6\text{B}_2\text{N}_2$ : C 54.87, H 9.54, N 4.57; found: C 54.89, H 9.62, N 4.07.

**Compound 8.** In a 5 mm quartz NMR tube, a pale-yellow solution of **1** (100 mg, 0.28 mmol) or **2** (114 mg, 0.28 mmol) and 2,5-bis(4-*N,N*-dimethylaminophenylethynyl)-thiophene (51.0 mg, 0.14 mmol) in 1.5 mL of THF was irradiated for 6 h at room temperature. The volatile components were removed *in vacuo*, and the brown residue was extracted with hexane (2 × 3 mL) followed by centrifugation. The brown hexane solution was decanted from the black residue and stored at  $-60^\circ\text{C}$  overnight to separate  $\text{Cr}(\text{CO})_6$  and an unidentified residue. The mother liquor was evaporated to dryness and **8** was isolated as an analytically pure yellow oily solid (60.2 mg, 61% yield).  $^1\text{H}$  NMR:  $\delta = 7.99$  (m, 4H, *H-m* of  $\text{C}_6\text{H}_4$ ), 7.64 (s, 2H,  $\text{C}_4\text{H}_2\text{S}$ ), 6.54 (m, 4H, *H-o* of  $\text{C}_6\text{H}_4$ ), 2.47 (s, 12H,  $\text{N}(\text{CH}_3)_2$ ), 0.46 (s, 36H,  $\text{Si}(\text{CH}_3)_3$ );  $^{13}\text{C}\{^1\text{H}\}$ -NMR:  $\delta = 150.9$  (s, C of  $\text{C}_6\text{H}_4$  bonded to  $\text{NMe}_2$ ), 137.8 (s, C of  $\text{C}_4\text{H}_2\text{S}$ ), 131.9 (s, *CH-m* of  $\text{C}_6\text{H}_4$ ), 130.4 (s, CH, of  $\text{C}_4\text{H}_2\text{S}$ ), 121.6 (s, *C-i* of  $\text{C}_6\text{H}_4$ ), 112.2 (s, *CH-o* of  $\text{C}_6\text{H}_4$ ), 39.8 (s,  $\text{N}(\text{CH}_3)_2$ ), 3.6 (s,  $\text{Si}(\text{CH}_3)_3$ );  $^{11}\text{B}\{^1\text{H}\}$ -NMR:  $\delta = 24.2$  (s). EI-MS  $m/z = 713$  ( $\text{M}^+$ ), 73 ( $\text{M} - \text{SiMe}_3^+$ ). Elemental analysis calcd. [%] for  $\text{C}_{36}\text{H}_{58}\text{Si}_4\text{B}_2\text{N}_4\text{S}$ : C 60.65, H 8.20, N 7.86; found: C 60.17, H 8.03, N 7.43.

**X-Ray Structure Determinations.** The crystallographic data of **6** and **7** were collected on a Bruker Apex diffractometer with a CCD area detector and graphite monochromated  $\text{Mo K}\alpha$  radiation. The structures were solved using direct methods, refined with the Shelx software package (G. Sheldrick, University of Göttingen 1997) and expanded using Fourier techniques. All non-hydrogen atoms were refined anisotropically. Hydrogen atoms were assigned idealized positions and were included in structure factor calculations.

**Crystal Data for 6.**  $\text{C}_{30}\text{H}_{50}\text{B}_2\text{N}_2\text{O}_2\text{Si}_4$ ,  $M_r = 604.70$ , yellow plate,  $0.30 \times 0.18 \times 0.07$  mm<sup>3</sup>, triclinic space group  $P\bar{1}$ ,  $a = 9.5049(11)$  Å,  $b = 13.4023(14)$  Å,  $c = 15.0311(18)$  Å,  $\alpha = 81.229(5)^\circ$ ,  $\beta = 72.047(5)^\circ$ ,  $\gamma = 79.572(5)^\circ$ ,  $V = 1781.9(4)$  Å<sup>3</sup>,  $Z = 2$ ,  $\rho_{\text{calcd}} = 1.127$  g·cm<sup>-3</sup>,  $\mu = 0.195$  mm<sup>-1</sup>,  $F(000) = 652$ ,  $T = 98(2)$  K,  $R_1 = 0.0529$ ,  $wR_2 = 0.1146$ , 10597 independent reflections [ $2\theta \leq 61.12^\circ$ ] and 361 parameters.

(34) Maher, J. M.; Beatty, R. P.; Cooper, N. J. *Organometallics* **1985**, *4*, 1354–1361.

(35) Haubold, W.; Kraatz, U. Z. *Anorg. Allg. Chem.* **1976**, *421*, 105–110.

(36) Batsanov, A. S.; Collings, J. C.; Fairlamb, I. J. S.; Holland, J. P.; Howard, J. A. K.; Lin, Z.; Marder, T. B.; Parsons, A. C.; Ward, R. M.; Zhu, J. J. *Org. Chem.* **2005**, *70*, 703–706.

**Crystal Data for 7.** C<sub>28</sub>H<sub>58</sub>B<sub>2</sub>N<sub>2</sub>Si<sub>6</sub>,  $M_r = 612.92$ , clear block,  $0.14 \times 0.07 \times 0.04 \text{ mm}^3$ , triclinic space group  $P\bar{1}$ ,  $a = 6.6063(9) \text{ \AA}$ ,  $b = 10.7222(14) \text{ \AA}$ ,  $c = 14.846(2) \text{ \AA}$ ,  $\alpha = 68.987(7)^\circ$ ,  $\beta = 82.634(7)^\circ$ ,  $\gamma = 77.599(7)^\circ$ ,  $V = 957.3(2) \text{ \AA}^3$ ,  $Z = 1$ ,  $\rho_{\text{calcd}} = 1.063 \text{ g} \cdot \text{cm}^{-3}$ ,  $\mu = 0.237 \text{ mm}^{-1}$ ,  $F(000) = 334$ ,  $T = 101(2) \text{ K}$ ,  $R_1 = 0.0587$ ,  $wR_2 = 0.1053$ , 3736 independent reflections [ $2\theta \leq 52.18^\circ$ ] and 172 parameters.

Crystallographic data have been deposited with the Cambridge Crystallographic Data Center as supplementary publication no. CCDC-722578 and 722579. These data can be obtained free of charge from The Cambridge Crystallographic Data Centre via [www.ccdc.cam.ac.uk/data\\_request/cif](http://www.ccdc.cam.ac.uk/data_request/cif).

**Computational Details.** The geometries of the molecules have been optimized with GAUSSIAN 03<sup>37</sup> using the gradient corrected hybrid functional B3LYP<sup>38</sup> in conjunction with the def2-SVP basis sets.<sup>39</sup> Energy minima and transition states have been verified by calculation of the Hessian matrices.<sup>40</sup> All stationary points which are reported here have only real frequencies and the transition states have one imaginary mode. Nucleus independent chemical shifts (NICS)<sup>41</sup> were evaluated using the gauge invariant atomic orbital (GIAO) approach at the GIAO-B3LYP/def2-SVP//B3LYP/def2-SVP level. Calculations of absorption spectra were accomplished using time-dependent density functional theory (TD-DFT)<sup>42</sup> method at the same level. The assignment of the excitation energies to the experimental bands was performed on the basis of the energy values and oscillator strengths. The B3LYP Hamiltonian was chosen because it was proven to provide accurate structures and reasonable UV–vis spectra for a variety of chromophores<sup>43</sup> including organometallic complexes.<sup>44</sup>

The atomic orbital occupations and the strength of the orbital interactions have been computed using the natural bond orbital (NBO) method.<sup>45</sup> The energies associated with the two-electron interactions have been computed according to the following equation:

$$\Delta E_{\phi\phi^*}^{(2)} = -n_{\phi} \frac{\langle \phi^* | \hat{F} | \phi \rangle^2}{\varepsilon_{\phi^*} - \varepsilon_{\phi}}$$

where  $\hat{F}$  is the DFT equivalent of the Fock operator and  $\phi$  and  $\phi^*$  are two filled and unfilled Natural Bond Orbitals having  $\varepsilon_{\phi}$  and  $\varepsilon_{\phi^*}$  energies, respectively;  $n_{\phi}$  stands for the occupation number of the filled orbital.

The nature of the interatomic interactions was investigated by means of the energy decomposition analysis (EDA) which was carried out with the program package ADF 2007.01.<sup>46</sup> For the EDA calculations, the geometries of the molecules were reoptimized at the gradient corrected DFT level using the exchange functional of Becke in conjunction with the correlation functional of Perdew (BP86).<sup>47</sup> Uncontracted Slater-type orbitals (STOs) were employed as basis functions for the SCF calculations.<sup>48</sup> The basis sets have triple- $\zeta$  quality augmented by two sets of polarization functions, that is, p and d functions for the hydrogen atoms and d and f functions for the other atoms. This level of theory is denoted as BP86/TZ2P. An auxiliary set of s, p, d, f, and g STOs was used to fit the molecular densities and to represent the Coulomb and exchange potentials accurately in each SCF cycle.<sup>49</sup> The EDA has proven to give comprehensive information about the nature of the bonding in main-group compounds and transition-metal complexes.<sup>50</sup> Details of the energy partitioning analysis can be found in the literature.<sup>50,51</sup>

**Acknowledgment.** We thank the Deutsche Forschungsgemeinschaft and the Fonds der Chemischen Industrie for financial support. R.M.W. and A.G.C. thank the EPSRC (U.K.) for PhD studentships. Part of the work has been carried out within the GRK 1221. We thank Catherine Heffernan and Dr. Alan M. Kenwright for obtaining some of the VT NMR spectra reported herein.

**Supporting Information Available:** CIF file for **6**, and **7**, Cartesian coordinates and total energies of all calculated compounds. Full list of authors for refs 37 and 46. This material is available free of charge via the Internet at <http://pubs.acs.org>.

JA902198Z

- (37) Frisch, M. J.; et al. *Gaussian03*; Gaussian, Inc.: Wallingford, CT, 2004.  
 (38) (a) Becke, A. D. *J. Chem. Phys.* **1993**, *98*, 5648. (b) Lee, C.; Yang, W.; Parr, R. G. *Phys. Rev. B* **1998**, *37*, 785. (c) Vosko, S. H.; Wilk, L.; Nusair, M. *Can. J. Phys.* **1980**, *58*, 1200.  
 (39) Weigend, F.; Alhrichs, R. *Phys. Chem. Chem. Phys.* **2005**, *7*, 3297.  
 (40) McIver, J. W.; Komornicki, A. K. *J. Am. Chem. Soc.* **1972**, *94*, 2625.  
 (41) (a) Schleyer, P. v. R.; Maerker, C.; Dransfeld, A.; Jiao, H.; Hommes, N. J. R. v. E. *J. Am. Chem. Soc.* **1996**, *118*, 6317. (b) Chen, Z.; Wannere, C. S.; Corminboeuf, C.; Puchta, R.; Schleyer, P. v. R. *Chem. Rev.* **2005**, *105*, 3842.  
 (42) (a) Casida, M. E. *Recent Developments and Applications of Modern Density Functional Theory*; Elsevier: Amsterdam, 1996; Vol. 4. (b) Casida, M. E.; Chong, D. P. *Recent Advances in Density Functional Methods*; World Scientific: Singapore, 1995; Vol. 1, p 155.  
 (43) For a review, see: Dreuw, A.; Head-Gordon, M. *Chem. Rev.* **2005**, *105*, 4009.  
 (44) Recent examples: (a) Andzelm, J.; Rawlett, A. M.; Orlicki, J. A.; Snyder, J. F. *J. Chem. Theory Comput.* **2007**, *3*, 870–877. (b) Nemykin, V. N.; Makarova, E. A.; Grosland, J. O.; Hadt, R. G.; Kuposov, A. Y. *Inorg. Chem.* **2007**, *46*, 9591. (c) Santi, S.; Orian, L.; Donoli, A.; Durante, C.; Bisello, A.; Ganis, P.; Cecon, A.; Crociani, L.; Benetollo, F. *Organometallics* **2007**, *26*, 5867. (d) Lage, M. L.; Fernández, I.; Mancheño, M. J.; Sierra, M. A. *Inorg. Chem.* **2008**, *47*, 5253.  
 (45) (a) Foster, J. P.; Weinhold, F. *J. Am. Chem. Soc.* **1980**, *102*, 7211. (b) Reed, A. E.; Weinhold, F. *J. Chem. Phys.* **1985**, *83*, 1736. (c) Reed, A. E.; Weinstock, R. B.; Weinhold, F. *J. Chem. Phys.* **1985**, *83*, 735. (d) Reed, A. E.; Curtiss, L. A.; Weinhold, F. *Chem. Rev.* **1988**, *88*, 899.

- (46) Baerends, E. J. et al. *Scientific Computing & Modelling NV*; Amsterdam: The Netherlands, 2007 ([www.scm.com](http://www.scm.com)).  
 (47) (a) Becke, A. D. *Phys. Rev. A* **1988**, *38*, 3098. (b) Perdew, J. P. *Phys. Rev. B* **1986**, *33*, 8822.  
 (48) Snijders, J. G.; Baerends, E. J.; Vernooijs, P. *At. Data Nucl. Data Tables* **1982**, *26*, 483.  
 (49) Krijn, J.; Baerends, E. J. *Fit Functions in the HFS-Method*; Vrije Universiteit Amsterdam: The Netherlands, 1984; Internal Report (in Dutch).  
 (50) (a) Frenking, G.; Wichmann, K.; Fröhlich, N.; Loschen, C.; Lein, M.; Frunzke, J.; Rayón, V. M. *Coord. Chem. Rev.* **2003**, *238–239*, 55. (b) Lein, M.; Frenking, G. *Theory and Applications of Computational Chemistry: The First 40 Years*; Dykstra, C. E., Frenking, G., Kim, K. S., Scuseria, G. E., Eds.; Elsevier: Amsterdam, 2005; p 291. (c) Esterhuysen, C.; Frenking, G. *Theor. Chem. Acc.* **2004**, *111*, 81. (d) Kovács, A.; Esterhuysen, C.; Frenking, G. *Chem.–Eur. J.* **2005**, *11*, 1813. (e) Krapp, A.; F. M.; Bickelhaupt; Frenking, G. *Chem.–Eur. J.* **2006**, *12*, 9196. (f) Fernández, I.; Frenking, G. *Chem.–Eur. J.* **2006**, *12*, 3617. (g) Fernández, I.; Frenking, G. *Faraday Discuss.* **2007**, *135*, 403. (h) Fernández, I.; Frenking, G.; Uggerud, E. *Chem.–Eur. J.* **2009**, *15*, 2166.  
 (51) (a) Bickelhaupt, F. M.; Baerends, E. J. *Rev. Comput. Chem.* **2000**, *15*, 1. (b) te Velde, G.; Bickelhaupt, F. M.; Baerends, E. J.; van Gisbergen, S. J. A.; Fonseca Guerra, C. J.; Snijders, G.; Ziegler, T. *J. Comput. Chem.* **2001**, *22*, 931.